GEOMETRY EFFECTS ON SOUND IN POROUS MEDIA

A. CORTIS AND D.M.J. SMEULDERS
Delft University of Technology, PO Box 5028, 2600 GA Delft, The Netherlands

D. LAFARGE
LAUM, UMR 6613, Av. O. Messiaen, 72017, Le Mans, France

AND

M. FIRDAOUSS AND J.L. GUERMOND
LIMSI, UPR 3251 (CNRS), BP 133, 91403 Orsay, France

Abstract. The problem of sound propagation in rigid porous media is investigated. Two so-called scaling functions are introduced to describe the dynamic viscous and thermal interaction of the pore fluid and the porous structure. These scaling functions are characterized by the viscous and thermal permeabilities k_0 and k_0', the viscous and thermal tortuosities α_∞, α_0, and α_0', and the characteristic length scales Λ and Λ'. These parameters can be numerically evaluated from steady-state descriptions. For a pore geometry consisting of an arrangement of cylinders, the characteristic parameters are presented. The full microscopic dynamic flow and heat problems for this configuration were solved, averaged, and compared with the scaling functions. We found that for this configuration the scaling functions gave an accurate description of the oscillatory flow and heat phenomena.

1. Introduction

Sound propagation in porous media is of importance in many fields of engineering science. In air-filled sound absorbing materials, the frequency dependence of the compressibility varies from isothermal at low frequencies to adiabatic in the high-frequency regime. Similarly, the frequency dependence of the gas density, which can be described in terms of dynamic flow permeability or in terms of dynamic frame tortuosity, varies from viscosity-dominated at low frequencies to inertia-dominated in the high-frequency

regime. The understanding of such behaviour in equally important for the oil industry, where acoustic borehole logging is commonly practiced. A borehole is drilled in a potential hydrocarbon reservoir and probed with an acoustic tool. The inversion process comprises the delineation of the reservoir properties from the acoustic signals, and is complicated because of the inherent inhomogeneity of the reservoir with its multiple inclusions and microcracks on the microscale. On the macroscale, where the measurements are performed, these inhomogeneities affect the viscous and thermal behaviour of the porous fluid-solid system. This work presents a numerical study on the macroscopic dynamic properties of a schematic rigid porous medium, starting from the microscopic geometry of the pore space.

2. Theory

The process of sound propagation in gas-filled rigid porous media can be characterized by a complex-valued tortuosity and compressibility. These two so-called scaling functions are frequency-dependent and governed by the microgeometry of the pores. The linear (i.e., small-amplitude) response of the pore fluid to a macroscopic pressure gradient $\nabla\langle\hat{p}\rangle e^{i\omega t}$ is usually described in terms of the macroscopic fluid velocity $\langle\hat{\mathbf{v}}\rangle e^{i\omega t}$ and the dynamic tortuosity $\alpha(\omega)$ (Johnson et al. 1987):

$$i\omega\alpha(\omega)\rho_f\langle\hat{\mathbf{v}}\rangle = -\nabla\langle\hat{p}\rangle, \tag{1}$$

where the dynamic tortuosity takes into account the viscous and inertial interaction of air with the porous frame. The combination $\alpha(\omega)\rho_f$ is sometimes called the dynamic gas density. The symbol $\langle\rangle$ denotes an intrinsic air-phase average. An alternative formulation is based on a dynamic extension of Darcy's law (Lévy 1979, Auriault et al. 1985):

$$\frac{\eta\phi}{k(\omega)}\langle\hat{\mathbf{v}}\rangle = -\nabla\langle\hat{p}\rangle, \tag{2}$$

where $k(\omega)$ is the dynamic permeability, ϕ is the porosity, and η the dynamic viscosity. This means that $\alpha(\omega)$ and $k(\omega)$ are not independent: $\alpha(\omega) = -i\alpha_\infty k_0\omega_c/\omega k(\omega)$, where we have introduced a characteristic frequency $\omega_c = \eta\phi/\alpha_\infty k_0\rho_f$ with k_0 the stationary Darcy permeability. Locally, $\hat{\mathbf{v}}$ and $\hat{p}$ have to satisfy the unsteady Stokes equation for incompressible media:

$$i\omega\rho_f\hat{\mathbf{v}} = -\nabla\hat{p} + \eta\nabla^2\hat{\mathbf{v}}. \tag{3}$$

On the basis of a microstructural approach, Auriault et al. (1985) and Johnson et al. (1987) proved that for high frequencies

$$\lim_{\omega\to\infty}\alpha(\omega) = \alpha_\infty\left[1 + (1-i)\frac{\delta(\omega)}{\Lambda}\right], \tag{4}$$

where α_∞ is the so-called tortuosity, $\delta(\omega)$ is the viscous boundary layer thickness $\sqrt{2\eta/\rho_f\omega}$, and Λ is a viscous length scale. For a porous material consisting of an ensemble of parallel identical tubes, for example, Λ equals the radius of those tubes.

For low frequencies, we simply find that $k(\omega) \rightarrow k_0$. A straightforward analytical scaling function was proposed by Johnson et al. (1987) which satisfies both high- and low-frequency limits:

$$\alpha(\omega) = \alpha_\infty[\ 1 - i\frac{\omega_c}{\omega}F(\omega)\ ], \tag{5}$$

where $F(\omega) = \sqrt{1 + \frac{1}{2}iM\frac{\omega}{\omega_c}}$, with M the so-called similarity parameter $8k_0\alpha_\infty/\phi\Lambda^2$.

Following Champoux & Allard (1991), we write the mass continuity law of a perfect gas to address the thermal dissipation problem:

$$i\omega\frac{\beta(\omega)}{\gamma\langle p\rangle}\langle\hat{p}\rangle = -\nabla\cdot\langle\hat{\mathbf{v}}\rangle, \tag{6}$$

where $\beta(\omega)$ is the reduced dynamic incompressibility $\gamma\langle p\rangle/K_f(\omega)$, with γ the specific heat ratio, and $K_f(\omega)$ the dynamic compressibility. Locally, the temperature equation for a perfect gas has to be satisfied:

$$i\omega\rho_f c_p\hat{T} = i\omega\hat{p} + \lambda_g\nabla^2\hat{T}. \tag{7}$$

Here, the specific heat at constant pressure is denoted by c_p, λ_g is the thermal conductivity, and $\hat{T}$ is the excess temperature. Introducing the characteristic thermal frequency $\omega_c' = a_g\phi/k_0'$, with k_0' the stationary thermal permeability and a_g the thermal diffusivity $\lambda_g/\rho_f c_p$, a straightforward analytical scaling function was proposed by Champoux & Allard (1991) to satisfy both the high-frequency adiabatic limit and the low-frequency isothermal limit:

$$\beta(\omega) = \gamma - (\gamma-1)[\ 1 - i\frac{\omega_c'}{\omega}F'(\omega)\ ]^{-1}, \tag{8}$$

where $F'(\omega) = \sqrt{1 + \frac{1}{2}iM'\frac{\omega}{\omega_c'}}$, with M' the thermal similarity parameter $8k_0'/\phi\Lambda'^2$. A thermal lengthscale Λ' is introduced here. The viscous and thermal behaviour can elegantly be described by means of the relaxation functions $\chi(\omega) = 1 - \alpha_\infty/\alpha(\omega)$ and $\chi'(\omega) = (\beta(\omega)-1)/(\gamma-1)$. They show similar behaviour over the entire frequency regime and they represent the so-called Johnson-Allard (JA) model. We will also consider the low-frequency exension of this JA-model, suggested by Pride et al. (1993). Here

the functions $F(\omega)$ and $F'(\omega)$ are defined as:

$$F(\omega) = 1 - p + p\sqrt{1 + \frac{1}{2} i \frac{M}{p^2} \frac{\omega}{\omega_c}}, \tag{9}$$

$$F'(\omega) = 1 - p' + p'\sqrt{1 + \frac{1}{2} i \frac{M'}{p'^2} \frac{\omega}{\omega'_c}}, \tag{10}$$

where $p = M/4(\alpha_0/\alpha_\infty - 1)$ and $p' = M'/4(\alpha'_0 - 1)$, with α_0 and α'_0 the low-frequency viscous and thermal equivalents of the tortuosity. This model will be referred to as the Pride model.

3. Numerical computations

Numerical computations were performed on a 2-D configuration of solid cylinders surrounded by gas drawn in the upper left corners of Figs. 1 and 2. The unit cell used in the computations has identical width and height $B = H = 2L$. The radius of the cylinders is $r = 0.7136L$, corresponding to a cell porosity $\phi = 0.60$. Using the SEPRAN finite-element package (Cuvelier et al. 1986), we computed α_∞, α_0, α'_0, Λ, Λ', k'_0, and k_0. The results are presented in Table 1. It was shown by Johnson et al. (1987) that $\alpha_\infty = \langle|\mathbf{v}_\infty|^2\rangle/|\langle\mathbf{v}_\infty\rangle|^2$, and that $2/\Lambda = \int |\mathbf{v}_\infty|^2 dS/\int |\mathbf{v}_\infty|^2 dV$, where the latter integral describes a velocity-weighted surface-to-volume ratio. The velocity field $\mathbf{v}_\infty = \nabla\psi$, limiting the oscillatory viscous flow for the high–frequencies regime, follows from the potential problem $\nabla^2\psi = 0$, with Neumann boundary conditions on the fluid–solid interface and periodicity on the inlet–outlet surfaces, i.e., the sides of the unit cell in this case. Furthermore, we computed k_0 by solving the Stokes problem $\eta\nabla^2\mathbf{v}_0 - \nabla p + \mathbf{e} = 0$, and $\nabla \cdot \mathbf{v}_0 = 0$, the quantity $\mathbf{e}$ being a unit force vector. No–slip boundary conditions at the pore walls, and periodicity of $\mathbf{v}_0$ and p were prescribed.

The thermal parameters can be expressed as follows: $\alpha'_0 = \langle T_0^2\rangle/\langle T_0\rangle^2$, and $2/\Lambda' = \int dS/\int dV$. This means that both α'_0 and k'_0 can be computed from the problem $\nabla^2 T_0 + e = 0$, where e is the thermal scalar equivalent of the unit force vector in the flow problem. Dirichlet boundary conditions on the fluid–solid surface, and periodicity on the inlet–outlet boundaries were used for T_0.

The full dynamic flow problem (3) was solved using a finite-element method developed by Guermond (Firdaouss et al. 1999). The full dynamic heat problem (7) was solved using the SEPRAN package. Results are presented in Figs. 1 and 2, where we plotted the two relaxation functions $\chi(\omega)$ and $\chi'(\omega)$. The shape of both scaling functions is identical. We notice that a perfect agreement between the numerical computations and the Pride

ϕ	k_0/L^2	α_0	α_∞	Λ/L	k_0'/L^2	α_0'	Λ'/L
0.6000	0.0184	1.7301	1.4105	0.7186	0.0505	1.2761	1.0705

TABLE 1. *Characteristic parameters.*

model can be found for both the flow and the heat problem. The JA–model gives a reasonable prediction of the numerical results, but shows some deviations in the rollover frequency zone. It was suggested previously that the scaling functions are accurate for a wide range of morphologies (Johnson et al. 1987), but that they break down for more extreme configurations where the pore flow channels contain sharp–edged intrusions (Firdaouss et al. 1999).

4. Conclusions

For a cylindrical pore geometry we have numerically computed the characteristic parameters determining the scaling functions defined by Johnson–Allard and Pride et al. These scaling functions were compared with a full solution of the microscopic dynamic flow and heat problems. An excellent agreement was found for the Pride model, whereas the Johnson model did show some minor deviations. We remark that the shape of the scaling functions for flow and heat are identical, due to the similarity between the dissipation processes in the viscous and thermal boundary layers.

References

1. Champoux, Y. and Allard, J.-F. 1991, 'Dynamic tortuosity and bulk modulus in air-saturated porous media'. *J. Appl. Phys.* **70**, 1975–1979.
2. Cuvelier, C., van Steenhoven, A.A. and Segal, G. 1986, 'Finite Element Methods and Navier-Stokes Equations'. Reidel.
3. Firdaouss, M., Guermond, J.L., Lafarge, D., Smeulders, D.M.J. 1999, 'Sound propagation in gas–filled rigid framed porous media: effect of cusped pore geometries'. *Bolletino di Geofisica* **40**, 80–81.
4. Johnson, D.L., Koplik, J. and Dashen, R. 1987, 'Theory of dynamic permeability and tortuosity in fluid-saturated porous media'.*J. Fluid Mech.* **176**, 379–402.
5. Pride, S.R., Morgan, F.D. and Gangi, A.F. 1993, 'Drag forces of porous-medium acoustics'. *Phys. Rev. B* **47**, 4964–4978.
6. Lévy, T. 1979, 'Propagation of waves in a fluid–saturated porous elastic solid'. *Int. J. Engng Sci.* **17**, 1005–1014.
7. Auriault, J.L., Borne, L. and Chambon, R. 1985, 'Dynamics of porous saturated media, checking of the generalized law of Darcy'. *J. Acous. Soc. Am.* **77**, 1641–1650.

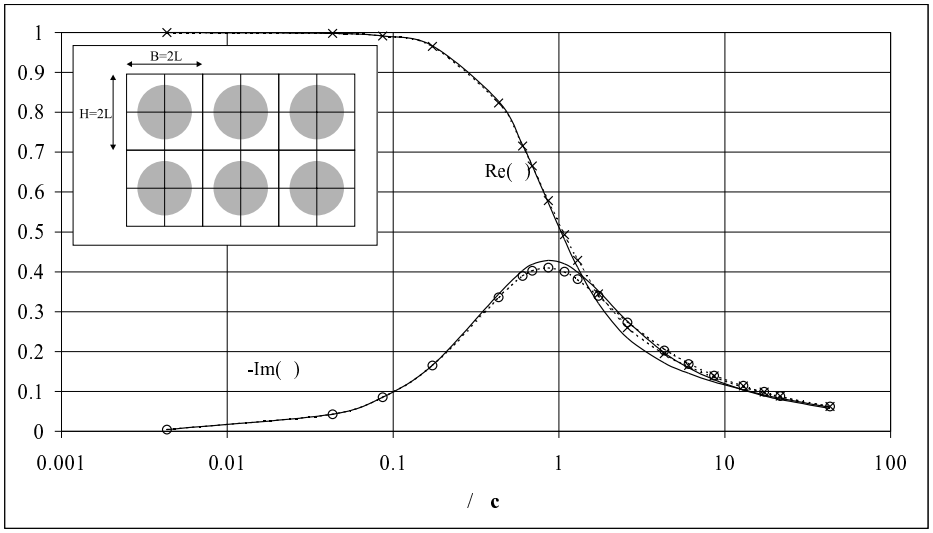

Figure 1. Viscous relaxation function vs dimensionless frequency ω/ω_c for an arrangement of solid cylinders surrounded by fluid. Crosses and circles represent direct numerical simulations. The solid line represents Johnson's model and the dashed line Pride's model.

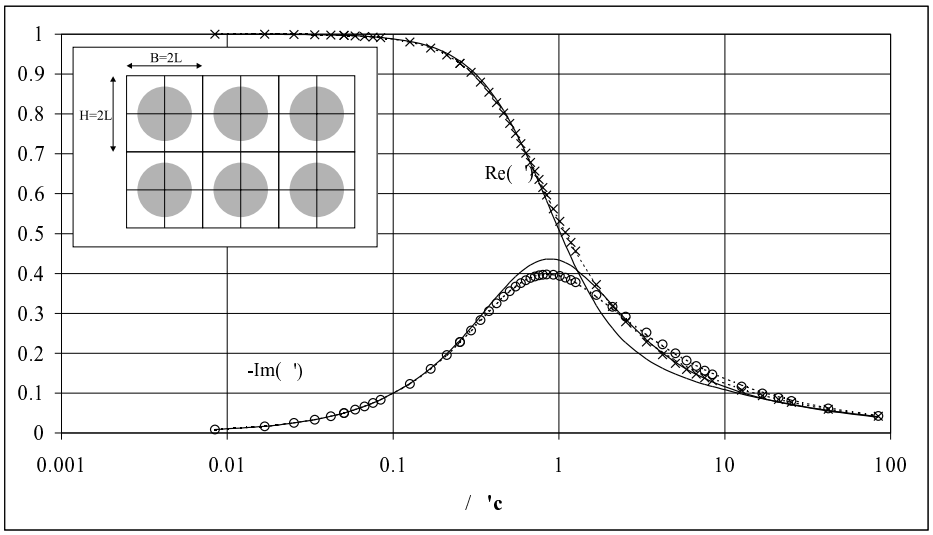

Figure 2. Thermal relaxation function vs dimensionless frequency ω/ω_c' for an arrangement of solid cylinders surrounded by fluid. Crosses and circles represent direct numerical simulations. The solid line represents Johnson's model and the dashed line Pride's model.